

# Differential Distributions for NLO Analyses of Charged Current Neutrino-Production of Charm

S. Kretzer<sup>1</sup>, D. Mason<sup>2</sup>, F. Olness<sup>3</sup>

<sup>1</sup>*Department of Physics and Astronomy, Michigan State University, East Lansing, MI 48824*

<sup>2</sup>*Department of Physics, University of Oregon, Eugene, OR 97403*

<sup>3</sup>*Department of Physics, Southern Methodist University, Dallas, TX 75275-0175*

## Abstract

Experimental analyses of charged current deep inelastic charm production – as observed through dimuon events in neutrino-iron scattering – measure the strangeness component of the nucleon sea. A complete analysis requires a Monte Carlo simulation to account for experimental detector acceptance effects; therefore, a fully differential theoretical calculation is necessary to provide complete kinematic information. We investigate the theoretical issues involved in calculating these differential distributions at *Next-Leading-Order* (NLO). Numerical results are presented for typical fixed target kinematics. We present a corresponding FORTRAN code suitable for experimental NLO analysis.

## 1 Introduction

Recent sets of global parton distribution functions (PDFs) [1–4] have reached a sufficiently high level of accuracy that quantization and propagation of statistical errors have become important issues [5]. It is, therefore, even more unsettling that the strange quark PDF,  $s(x, Q^2)$ , remains a mystery [6] without a fully consistent picture emerging from the comparative analysis between neutrino and muon structure functions [7–9], opposite sign dimuon production in  $\nu Fe$ -DIS [8–16], or the recently measured parity violating structure function  $\Delta x F_3$  [6, 17]. Given the high precision of the non-strange PDF components, this situation for  $s(x, Q^2)$  is unacceptable both in terms of our understanding of the nucleon structure, and for our ability to use precise flavor information to make predictions for present and future experiments.

For extracting the strange quark PDF, the dimuon data provide the most direct determination. The basic channel is the weak charged current process  $\nu s \rightarrow \mu^- c X$  with a subsequent

charm decay  $c \rightarrow \mu^+ X'$ . These events provide a direct probe of the  $sW$ -vertex, and hence the strange quark PDF.<sup>1</sup> For this reason, fixed-target neutrino dimuon production will provide a unique perspective on the strange quark distribution of the nucleon in the foreseeable future. Besides, HERA provides a large dynamic range in  $Q^2$  for the CP conjugated process  $e^- \bar{s} \rightarrow \bar{\nu} c$  which is valuable for testing the underlying QCD evolution [18, 19]. Within the HERMES experimental program [20] the flavor structure of the polarized and unpolarized sea are studied from semi-inclusive DIS where DIS Kaon production has obvious potential to probe strangeness. Thus, HERA and HERMES can complement fixed-target neutrino dimuon data with information at different energies and from different processes; therefore, neutrino DIS serves for now as an important benchmark process to perform rigorous and refined comparisons between the experimental data and the theoretical calculations. In the long run, a high luminosity neutrino factory could, of course, considerably raise the accuracy of present day information from  $\nu$  DIS [21].

The theoretical calculations of inclusive charged current charm production have been carefully studied in the literature [8, 18, 22–27]. Additionally, the charm fragmentation spectrum has also been calculated in detail [16, 18]. While inclusive calculations are sufficient for many tasks, a comprehensive analysis of the experimental data at NLO requires additional information from the theoretical side. In charged current  $\nu$ -Fe charm production, the detector acceptance depends on the full range of kinematic variables:  $\{x, Q^2, z, \eta\}$ .<sup>2</sup> Here,  $x$  is the Bjorken- $x$ ,  $Q$  is the virtuality of the  $W$ -boson,  $z$  is the scaled energy of the charm after fragmentation, and  $\eta$  is charm rapidity. The theoretical task is, *mutatis mutandis*, not too different from the extraction of the neutral current charm structure function  $F_2^c$  as performed by the HERA experiments [28]; this analysis uses the theoretical calculation of the differential cross section [29] to extrapolate into regions of poor acceptance.

The organization of this paper is as follows. In Section 2, we discuss the key factors that influence the acceptance of the experimental detector. In Section 3, we review the theoretical calculation of the fully differential cross section at NLO in QCD [16]. In Section 4 we present numerical results for typical fixed target kinematics. Finally, in Section 5, we draw our conclusions.

---

<sup>1</sup>In contrast, single muon production only provides indirect information about  $s(x, Q^2)$  which must then be extracted from a linear combination of structure functions in the context of the QCD parton model.

<sup>2</sup>Azimuthal  $\phi$ -dependence is controlled to be flat by rotational symmetry around the axis of the boson-target frame. It is, therefore, not indicated.

## 2 Experimental Environment: $\nu Fe$ DIS

Dimuon events from neutrino charged current charm production can provide a clear set of events from which to study the strange sea. Their signature in a detector is a pair of oppositely charged muons and a hadronic shower originating from the same vertex. The second muon is produced in the semileptonic decay of the charmed particle. Detector geometry and applied cuts affect how these events are reconstructed, and must be corrected for when making measurements of the underlying charm production. These corrections require a cross section differential in variables in addition to the typical  $E_\nu, x$ , and  $Q^2$  or  $y$  of the charged current cross section.

To separate dimuon events from backgrounds a minimum energy requirement must be applied to the muon from charm decay. For the muon to be visible at all, it must first be energetic enough that it travels further in the detector than the particles which make up the hadronic shower. The background from muons from nonprompt decays of pions and kaons within the shower is large at low energy, and must also be reduced. Typically a cut on the charm decay muon's energy of a few GeV is applied to guarantee it be reconstructable, and to reduce the nonprompt backgrounds. The energy of the decay muon depends on the energy of the charmed meson from which it decays, and therefore depends on the fragmentation parameter  $z$ . In NLO, it also depends on the rapidity of the charmed quark, which maps onto the  $W$ -parton CMS scattering angle. A charmed meson with low  $z$ , and/or low rapidity will be less likely to pass a cut on the decay muon's energy than one with high  $z$  and maximal<sup>11</sup> rapidity. In addition, the linear construction of typical fixed target neutrino detectors can adversely affect the reconstruction of decay muons with large scattering angles. Considering these effects, it is important that the charm production cross section's dependence on both  $z$  and charm rapidity be understood to be able to model dimuon events and their detector acceptance properly.

Fig. 1 illustrates the effect of a decay muon energy and angle cut on  $z$  and rapidity acceptance at a particular  $E_\nu, x$ , and  $Q^2$  point. A toy monte carlo was constructed that generated charmed mesons with flat distributed  $z$  and charm rapidity, and decayed them into muons following [30]. Detector smearing effects were not included. The figure shows muon acceptance after a 5 GeV cut on energy, and a maximum scattering angle cut of 0.250 radians, as a function of  $z$  and charm rapidity for  $E_\nu = 80$  GeV,  $x = 0.1$ , and  $Q^2 = 10$  GeV<sup>2</sup>. The acceptance is a smooth function in both kinematic variables, but flattens out as  $z$  approaches 1 and rapidity approaches its maximum value. To properly correct for acceptance the cross

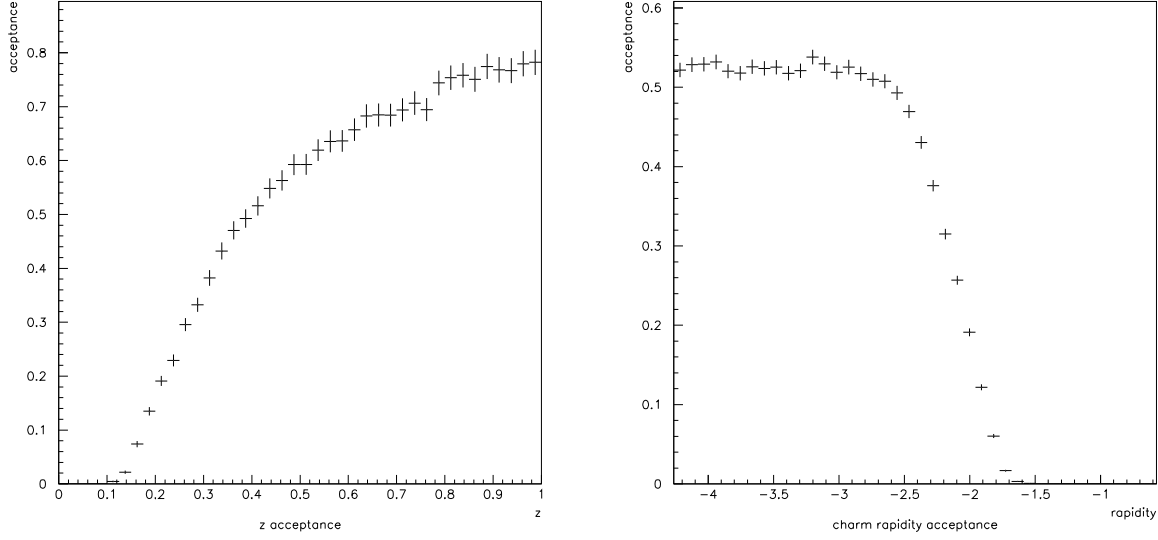


Figure 1: Relative acceptance  $\mathcal{A}(z, \eta)$  induced from typical kinematic cuts (as detailed in the text) on the decay-muon for  $E_\nu = 80$  GeV,  $x = 0.1$ ,  $Q^2 = 10$  GeV<sup>2</sup>.

section must be differential where the slope is nonzero, but in regions where the acceptance is flat, the dependence on these variables may be safely integrated out; i.e. we conclude that the integrated acceptance correction

$$\int dz d\eta [1 - \mathcal{A}(z, \eta)] \frac{d\sigma}{dx dQ^2 dz d\eta} \quad (1)$$

does not resolve any local deviations of  $d\sigma$  around some point  $z_0, \eta_0$  within a range where  $[\partial\mathcal{A}(z, \eta)/dz] \times (z - z_0)$  and  $[\partial\mathcal{A}(z, \eta)/d\eta] \times (\eta - \eta_0)$  are smaller than the typical MC accuracy. In our example, these conditions are safely met within a range of, say, 1 unit in rapidity and 0.2 units in  $z$  away from the phase space boundary.

### 3 Differential Distributions at NLO

Recorded charged-current charm production rates must be corrected for the detector acceptance which, as discussed above, depends on the full range of kinematic variables:  $\{x, Q^2, z, \eta\}$ .<sup>2</sup> Therefore, we must obtain the NLO theoretical cross section which is completely differential in all these variables.

While  $x$  and  $Q^2$  are fixed by the energy and angle of the scattered muon, the variables  $z$  and  $\eta$  relate to the center-of-mass-system (CMS) phase space of the hard partonic scattering event, which at *Leading-Order* (LO) is  $W^+ s' \rightarrow c$ . At NLO, the quark-initiated process ( $W^+ s' \rightarrow c$ ) receives virtual and real corrections, and we encounter a new gluon-initiated

process,  $W^+g \rightarrow c\bar{s}'$ . Neglecting bottom contributions,<sup>3</sup> we denote the CKM-rotated weak eigenstate with  $s'$ , which is defined as:

$$s' = |V_{s,c}|^2 s + |V_{d,c}|^2 d \quad (2)$$

Similarly, we will use

$$g' \equiv g (|V_{s,c}|^2 + |V_{d,c}|^2) \quad (3)$$

to denote its QCD evolution partner, *i.e.*,  $ds'/d\ln Q^2 = s' \otimes P_{qq} + g' \otimes P_{qg}$ .

The NLO 2-particle partonic phase space in  $N = 4 + 2\epsilon$  dimensions (appropriate for a single charm quark of mass  $m_c$ , plus a massless gluon or strange quark) is:

$$\int d\text{PS}_2 = \frac{1}{8\pi} \frac{s - m_c^2}{s} \frac{1}{\Gamma(1 + \epsilon)} \left[ \frac{(s - m_c^2)^2}{4\pi s} \right]^\epsilon \int_0^1 [\hat{y}(1 - \hat{y})]^\epsilon d\hat{y} \quad (4)$$

Note that there is only one independent variable;<sup>4</sup> In Eq. (4), this has been chosen to be  $\hat{y} \equiv (1 + \cos\theta^*)/2$ , with  $\theta^*$  being the  $W^\pm$ -parton CMS scattering angle.

The expression for the phase space in Eq. (4) leaves us two options for computing the cross section: i) we can either integrate over the entire phase space, or ii) we can compute a singly-differential distribution.

### 3.1 Singly Differential Distributions

We can construct any singly-differential cross section as follows. If the variable  $\Xi$  stands for any kinematic variable that can be expressed through  $\hat{y}$  and partonic CMS energy  $\hat{s}$ , we can easily obtain the differential cross section with respect to  $\Xi$  with the appropriate Jacobian via the relation:  $d\sigma/d\Xi = (d\sigma/d\hat{y}) (d\hat{y}/d\Xi)$ . As above,  $\hat{y} \equiv (1 + \cos\theta^*)/2$  and the partonic CMS energy is given by:

$$\hat{s} = \frac{Q^2}{\xi'} \left( 1 - \xi' + \frac{m_c^2}{Q^2} \right) \quad , \quad (5)$$

with  $\xi'$  defined below in (8). In our case, we consider a distribution singly-differential in  $\zeta$ , the partonic fragmentation variable

$$\zeta \equiv \frac{p_c \cdot P_N}{q \cdot P_N} = \frac{\hat{y}(\hat{s} - m_c^2) + m_c^2}{\hat{s}} \quad (6)$$

---

<sup>3</sup>We can safely neglect the bottom quark-initiated contributions as these are suppressed both due to the bottom-quark mass, and also by the Cabibbo-Kobayashi-Maskawa (CKM) matrix element.

<sup>4</sup>To count the degrees-of-freedom, we have  $2 \times 4$  momentum coordinates, minus 2 mass shell conditions, minus 4 energy momentum conserving conditions, minus 1 rotational symmetry around the CMS axis.

which reduces to the scaled energy of the unobservable (colored) charm quark,  $\zeta = E_c/E_W$ , in the target rest frame. After fragmentation the observable (colorless) charm hadron (collectively labeled a  $D$ -meson) carries some smaller energy  $z = E_D/E_W < \zeta$ .

The unobservable variable  $\zeta$  is convoluted with a fragmentation function to compute the observable CC DIS hadronic charm structure functions:

$$\begin{aligned} \mathcal{F}_i^c(x, z, Q^2) &= s'(\xi, \mu_F^2) D_c(z) \\ &+ \frac{\alpha_s(\mu_F^2)}{2\pi} \int_{\xi}^1 \frac{d\xi'}{\xi'} \int_{\max(z, \zeta_{\min})}^1 \frac{d\zeta}{\zeta} \left[ H_i^q(\xi', \zeta, \mu_F^2, \lambda) s'(\frac{\xi}{\xi'}, \mu_F^2) \right. \\ &\left. + H_i^g(\xi', \zeta, \mu_F^2, \lambda) g'(\frac{\xi}{\xi'}, \mu_F^2) \right] D_c(\frac{z}{\zeta}) \quad , \end{aligned} \quad (7)$$

In Eq. (7),  $D_c(z)$  is the fragmentation function (often parameterized in the form of Peterson *et al.* [31]),  $z$  is the scaled charm hadron energy,  $\xi = x(1 + m_c^2/Q^2)$ ,  $\zeta_{\min} = m_c^2/\hat{s} = (1 - \lambda)\xi'/(1 - \lambda\xi')$  and  $\lambda = Q^2/(Q^2 + m_c^2)$ .

The outer convolution integral over the variable

$$\xi' = \frac{Q^2}{2p_{s,g} \cdot q} \left( 1 + \frac{m_c^2}{Q^2} \right) = \frac{Q^2 + m_c^2}{\hat{s} + Q^2} \quad (8)$$

folds in the quark and gluon PDFs. We take the factorization scale  $\mu_F$  used in the PDFs equal to the renormalization scale  $\mu_R$  used in  $\alpha_s(\mu_R)$ . We find it convenient to normalize our  $\mathcal{F}_i^c$  relative to the conventional CC DIS structure functions  $F_i^c$  as follows:  $\mathcal{F}_1^c \equiv F_1^c$ ,  $\mathcal{F}_3^c \equiv F_3^c/2$ ,  $\mathcal{F}_2^c \equiv F_2^c/2\xi$ . We adopt the standard normalization of semi-inclusive structure functions as implicitly defined through

$$F_i(x, Q^2) = \int \left( \prod_{\alpha \in \{\Xi\}} d\alpha \right) F_i(x, Q^2, \{\Xi\}) \quad (9)$$

with  $\{\Xi\}$  any set of kinematic variables.

The form of the hard-scattering coefficients,  $H_i^{q,g}$ , can be found in [16, 18]. These hard-scattering coefficients,  $H_i^{q,g}$ , are mathematical distributions containing both Dirac- $\delta$  and (generalized) *plus* distributions arising from the soft singularities and mass singularities present in the NLO QCD calculation.<sup>5</sup> To map these distributions into C-numbers, smooth test functions are required; normally, it is the parton distribution functions and the fragmentation functions that serve as these smooth test functions. Convolutions over *both*  $\xi'$  and  $\zeta$

---

<sup>5</sup>In this article, the term *distributions* may denote either kinematic or mathematical ones; the individual meaning will be clear from the context.

are necessary to guarantee C-number results for the hadronic structure function on the left-hand-side (LHS) of Eq. (7); the convolution over  $\xi'$  folds in the PDFs, and the convolution over  $\zeta$  folds in the fragmentation function.

In light of the above discussion, we clearly see that if we require structure functions which are fully differential in all four variables, such as  $\mathcal{F}_i^c(x, Q^2, z, \eta)$  which is required to compute the experimental detector acceptance, we will be left with unphysical Dirac- $\delta$  and *plus* distributions. Let us note that we are facing a new problem that is intimately related to the single-charm kinematics of charged-current DIS. There is no direct lesson to be learnt from the pair-production kinematics of the well-understood neutral-current case [29] where the phase space has more degrees of freedom. We now turn to address this question.

### 3.2 Fully Differential Distributions

Suppose we wish to compute the structure function which is differential in four variables. As a specific example, we will choose  $\mathcal{F}_i^c(x, Q^2, z, p_T^{c,*})$  where  $p_T^{c,*}$  is the transverse momentum of the charm particle in the boson-parton CMS frame. From Eq. (4) and Eq. (7) we will find  $\mathcal{F}_i^c(x, Q^2, z, p_T^{c,*})$  contains mathematical distributions of the form:  $\delta(p_T^{c,*} - \overline{p_T^{c,*}})$  and  $1/(p_T^{c,*} - \overline{p_T^{c,*}})_+$ , where  $\overline{p_T^{c,*}} = \sqrt{(1-\zeta)(\zeta\hat{s} - m^2)}$ . The  $\delta$ -function distributions arise from the diagrams that have LO ( $2 \rightarrow 1$ ) kinematics, whereas the plus-distributions arise from diagrams with NLO ( $2 \rightarrow 2$ ).

In principle, C-numbers are ultimately obtained from the  $\mathcal{F}_i^c(x, Q^2, z, p_T^{c,*})$  distribution after convolution with a smooth detector-resolution function in a MC program. While such an approach may work in principle, there are many inherent difficulties trying to interface mathematical  $\delta$ -function distributions and plus-distributions with a complex detector simulation MC program.

In the next sections, we first look at the source of the singularities which appear in the theoretical calculation, and then find a means to extract the relevant distributions in an expeditious manner.

### 3.3 Resumming Soft Gluons and the Sudakov Form Factor

As mentioned above, if we compute the fully differential  $\mathcal{F}_i^c(x, Q^2, z, \eta)$ , or equivalently  $\mathcal{F}_i^c(x, Q^2, z, p_T^{c,*})$ , the final state is over-constrained and this yields an unphysical delta-

function distribution in the observable cross section. While such a distribution will yield sensible results for any integrated observable, the full differential distribution  $d\sigma/dxdQ^2dzdp_T$  will contain unphysical singularities.

This affliction is the limitation of our fixed-order perturbation theory; were we able to perform an all-orders calculation, such singular distributions would never occur—as is appropriate for a physical process. In our particular case, the singular behavior of our fixed-order perturbation theory would be resolved were we to include soft gluon emissions as in the familiar Sudakov process. We will briefly review the Sudakov resummation of soft gluon emissions off massless particles, and then assess how best to work with  $\mathcal{F}_i^c(x, Q^2, z, \eta)$  for non-zero charm mass.

One of the early resummations of the QCD logarithms of the form  $\ln Q^2/q_T^2$  arising from soft gluon emissions was performed by Dokshitzer, Diakonov and Troian (DDT) [32]. They obtained the leading-log Sudakov form factor which can be written generically as:

$$S(q_T, Q) = \exp \left\{ - \int_{q_T^2}^{Q^2} \frac{d\mu^2}{\mu^2} \frac{\alpha_s(\mu)}{\pi} \left( A \ln \frac{Q^2}{\mu^2} + B \right) \right\}$$

where  $q_T = -p_T/z$  is the transverse momentum of a massless particle produced in DIS divided by fragmentation- $z$ . The net result of this Sudakov form factor is to smear the  $p_T$  distribution from a singular delta-function, to a more physical form—often taken to be a Gaussian.<sup>6</sup>

The phenomenological approach we will take in this paper is divided into two steps.

1. We regularize the NLO calculation of  $\mathcal{F}_i^c(x, Q^2, z, \eta)$  to provide a numerical distribution free of delta-functions and plus-distributions.
2. This result is input to a Monte Carlo (MC) calculation where the additional effects, including iterated soft gluon emissions, is modeled by a Gaussian distribution that has been fit to data.

---

<sup>6</sup>There are a number of different implementations of this formalism. In the Collins-Soper-Sterman (CSS) formalism [33], this process is separated into a perturbative and a non-perturbative Sudakov form factor. The perturbative Sudakov form factor ( $\mathcal{S}^P$ ) represents a formal resummation of the soft-gluon emissions. The non-perturbative Sudakov form factor ( $\mathcal{S}^{NP}$ ) is introduced to deal with the singularities in the perturbative coupling at  $\alpha_s(\mu)$  at  $\mu = \Lambda_{QCD}$  [41, 42]. Separately, Contopanagos and Sterman [34] developed a Principal Value Resummation which provides a prescription for regularizing this singularity. More recently, Ellis and Veseli [35] derived a technique that operates purely in  $q_T$  without resorting to a Bessel transform to b-space.



To ensure that we have an accurate representation of the differential distribution suitable for evaluating the experimental acceptance and extracting the strange-quark PDF, we need to verify that the net smearing due to step 1) and step 2) combine to yield the smearing measured by experiment.

The transverse momentum of charmed particles about the direction of the charm quark has been measured by the LEBC EHS collaboration [36], and by the neutrino emulsion experiment FNAL-E531 [37]. They fit to a Gaussian distribution:

$$\frac{dN}{dp_T^2} \sim e^{-p_T^2/\langle p_T^2 \rangle}$$

with  $\langle p_T^2 \rangle$  on the order of  $\sim 900$  MeV.

This observation implies that the details of the specific regularization procedure are inconsequential; they can simply be compensated by adjusting the smearing of the Monte Carlo so that the net smearing (regularization plus Monte Carlo) yield the experimental transverse momentum distribution. Effectively, this parameterizes the gluon resummation of the Sudakov form factor. In practice, we can proceed along items **a)** or **b)** of Section 3.4 and adjust the regularization parameters by either varying the  $\langle p_T^2 \rangle$  in the  $G$  function in Eq. (10) below, or by varying the bin width differential distribution. This cross-check ensures that we have an accurate representation of the differential distribution suitable for evaluating the experimental acceptance and extracting the strange-quark PDF.

We now discuss the implementation of this procedure in the following section.

### 3.4 Implementing the Fully Differential Distribution

As demonstrated above, the singular distributions are nothing but an unphysical artifact of regularized perturbation theory; for any physically observable quantity, these singularities will be smeared by soft gluon emission to yield physical C-number distributions [38, 39]. As the theoretical machinery of soft gluon resummation is not fully developed for semi-inclusive DIS heavy quark production, we will use a phenomenological approach.<sup>7</sup> There are two viable options that we have investigated.

- a) **Gaussian  $p_T$ -smearing:** We may smear the singular peak which appear in the differential structure functions.

---

<sup>7</sup>Note, the application of the Sudakov resummation to the case of semi-inclusive DIS heavy quark production is under current investigation; such an approach would be of use in a future very-high-statistics experiment where the detailed  $p_T$ -distribution could be measured.

- b) **Binning:** We may map the singular distributions onto C-numbers distributions by integrating over bins which reflect the finite resolution of the experimental detector.

We examine these possibilities in order.

### 3.4.1 Gaussian $p_T$ -smearing

We can implement Gaussian  $p_T$ -smearing by replacing the delta function  $\delta(p_T^{c,*} - \overline{p_T^{c,*}})$  with a narrow Gaussian distribution  $G(p_T^{c,*}, \overline{p_T^{c,*}}, \delta p_T^{c,*})$  centered about the perturbative value  $\overline{p_T^{c,*}}$ , and with a width of  $\delta p_T^{c,*}$ :<sup>8</sup>

$$G(p_T^{c,*}, \overline{p_T^{c,*}}, \delta p_T^{c,*}) = \frac{1}{\delta p_T^{c,*} \sqrt{\pi}} e^{\frac{-2(p_T^{c,*} - \overline{p_T^{c,*}})^2}{(\delta p_T^{c,*})^2}} \quad (10)$$

Once we have a smooth distribution in  $p_T^{c,*}$ , we can trivially switch to any other variable,  $\Xi$ , by applying the proper Jacobian:<sup>9</sup>

$$G(\Xi, \overline{\Xi}, \delta\Xi) = G(p_T^{c,*}, \overline{p_T^{c,*}}, \delta p_T^{c,*}) \times \frac{\partial \overline{p_T^{c,*}}}{\partial \Xi} \quad (11)$$

For non-zero  $\delta p_T^{c,*}$ , we pass C-numbers to the MC. In the limit  $\delta p_T^{c,*} \rightarrow 0$ , we have  $G(p_T^{c,*}, \overline{p_T^{c,*}}, 0) = \delta(p_T^{c,*} - \overline{p_T^{c,*}})$ , and the original mathematical (singular) distributions are recovered. In practice, a Gaussian smearing regularization of the  $H_i^{q,g}$  in Eq. (7) corresponds to a replacement

$$H_i^{q,g}(\xi', \zeta, \mu_F^2, \lambda) \rightarrow \overline{H}_i^{q,g}(\xi', \zeta, \mu_F^2, \lambda) = H_i^{q,g}(\xi', \zeta, \mu_F^2, \lambda) \times G(p_T^{c,*}, \overline{p_T^{c,*}}) \quad (12)$$

with  $\overline{p_T^{c,*}} \equiv \overline{p_T^{c,*}}(\xi', \zeta)$  understood as a function of  $\xi'$  and  $\zeta$ .

### 3.4.2 Finite Detector Resolution and Binning Distributions

An alternate approach is to map the singular distributions onto C-numbers distributions by integrating over bins which reflect a finite resolution of the detector. Additionally, this technique can avoid passing negative weights to the MC if the bin size is sufficiently large enough to allow the KLN theorem to effect its cancellations. This point will be further discussed in Section 4.

---

<sup>8</sup>Note, the actual normalization of the Gaussian is more subtle than shown here as the integration in  $p_T^{c,*}$  will be constrained by kinematic limitations. This complication is one reason that we do not implement this approach in practice.

<sup>9</sup>Note,  $G(\Xi, \overline{\Xi}, \delta\Xi)$  will not necessarily be a Gaussian.

In practice, the binning means that in Eq. (7) we make the replacement

$$H_i^{q,g}(\xi', \zeta, \mu_F^2, \lambda) \rightarrow \tilde{H}_i^{q,g}(\xi', \zeta, \mu_F^2, \lambda) = H_i^{q,g}(\xi', \zeta, \mu_F^2, \lambda) \times \Theta_{\Xi}(\xi', \zeta) \quad (13)$$

where the step function  $\Theta_{\Xi}(\xi', \zeta) = 1$  if  $\Xi \equiv \Xi(\xi', \zeta)$  is inside the bin  $\Delta\Xi$  over which to integrate, and zero otherwise. Note, this means that  $\Theta_{\Xi}(\xi', \zeta)$  is subject to the distribution prescriptions of the original  $H_i^{q,g}$  as given in Refs. [16, 18]; *i.e.*,  $\Theta_{\Xi}(\xi', \zeta)$  must be treated with care as a multiplicative factor to the non-singular “test-function” part of the  $H_i^{q,g}$ .

### 3.4.3 Practical Considerations

We will briefly comment why we favor implementing the binning of choice b) as opposed to the Gaussian  $p_T$ -smearing. For the present case of the charm transverse momentum,  $\Xi = p_T^{c,*}$ , (or equivalently, the charm rapidity  $\Xi = \eta$ ), Gaussian  $p_T$ -smearing leads to a integrable but delicately singular behavior near the boundary of phase space – which corresponds to the singular point of the distributions – unless we smear the  $p_T^{c,*}$  variable with a width  $\delta p_T^{c,*}$  as large as  $\sim m_c$ .

In the context of resummation of soft gluon emissions into the Sudakov form factor, the width  $\delta p_T^{c,*}$  should be tied to a scale characteristic of the soft processes within the hadron, possibly with a logarithmic growth [40]. For fixed-target neutrino DIS,  $p_T^{c,*} \sim m_c$  represents a comparatively large transverse momentum. Additionally, there is the complication of the normalization of the Gaussian given the constraints of the phase space boundaries.

Consequently, while the Gaussian  $p_T$ -smearing may have a simple intuitive interpretation, we find the second method of using finite width bins to be more economical in terms of CPU time and numerical stability. Results for this approach with  $\Xi$  identified with charm rapidity  $\eta$  will be presented in the next section.

## 4 Numerical Results

We have previously addressed in Section 3 the complication of mapping mathematical distributions onto C-number functions by the introduction of bins. We also encounter large and negative Sudakov logarithms close to the phase space boundary where, at fixed-order, soft single-gluon emission is enhanced. Let us, for illustration, consider the convolution of a plus-distribution  $1/(1-x)_+$ , and a sufficiently smooth and monotonically decreasing test

function  $f(x) > 0$ . Then, the integral

$$\int_{x_{\min}}^1 dx \frac{f(x)}{(1-x)_+} = \int_{x_{\min}}^1 dx \frac{f(x) - f(1)}{(1-x)} + f(1) \ln(1 - x_{\min}) \quad (14)$$

will be positive for  $x_{\min}$  not too close to 1. As in this simplified “toy” case, the Sudakov logarithms near the phase space boundary diverge in the limit of zero bin-width [ $x_{\min} \rightarrow 1$  in (Eq. (14))]; as we increase our resolution via narrow binning, we begin to resolve the unphysical  $\delta$ -functions and “plus-distributions.” Conversely, by using broad bins, we are effectively integrating over enough phase-space so that the KLN theorem ensures that we obtain positive physical results.

## 4.1 Kinematics for Rapidity Distributions

We now compute the normalized differential charm production cross section:

$$d\sigma_{\{x,y,z,\eta\}} \equiv \frac{d\sigma}{dx dy dz d\eta} \left[ \frac{2G_F^2 M_N E_\nu}{\pi \left(1 + \frac{Q^2}{M_W^2}\right)^2} \right]^{-1} \quad (15)$$

We can compute  $d\sigma_{\{x,y,z,\eta\}}$  from the master equation for the differential structure function, Eq. (7), with the binning procedure defined by Eq. (13). For our variables, we choose the set  $\{x, Q, z, \eta\}$  where  $\eta$  is the charm rapidity evaluated in the collinear ( $p_{\perp,W} = 0$ ) target rest frame.

In the partonic center of mass system, the charm rapidity is defined by:

$$\eta^* = \frac{1}{2} \ln \frac{E_c^* + p_{L,c}^*}{E_c^* - p_{L,c}^*} \quad (16)$$

and the other necessary variables are:

$$E_c^* = \frac{\hat{s} + m_c^2}{2\sqrt{\hat{s}}} \quad (17)$$

$$p_{L,c}^* = - \frac{\hat{s} - m_c^2}{2\sqrt{\hat{s}}} \cos \theta^* \quad (18)$$

$$\cos \theta^* = 1 - 2 \frac{(1 - \zeta)(1 - \lambda \xi')}{1 - \xi'} \quad (19)$$

We find the charm rapidity to be a convenient variable as the relation between the rapidity in the partonic center of mass system,  $\eta^*$  and the rapidity in collinear target rest frame  $\eta$

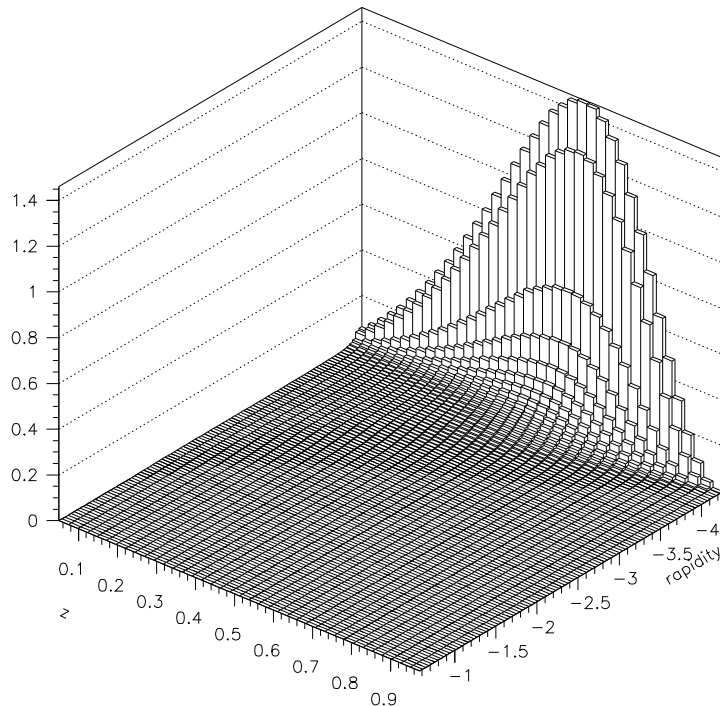


Figure 2: Binned differential distribution for CC neutrino-production of charm on an isoscalar target; the kinematics shown are for a typical wide-band beam on a fixed target:  $E_\nu = 80$  GeV,  $x = 0.1$ ,  $Q^2 = 10$  GeV<sup>2</sup>.

are related by a simple relation:

$$\eta = \eta^* + \frac{1}{2} \ln \left[ \frac{M_N^2}{Q^2} x \left( \frac{\xi}{\xi'} - x \right) \right] \quad (20)$$

We will use the collinear target rest frame as our reference frame since it is related to the laboratory frame by a simple spatial rotation which depends on an event-by-event basis on the kinematics of the leptonic vertex.

## 4.2 Tracking Down Sudakov Logarithms

In Fig. (2) and Fig. (3) we present results for kinematics typical of a wide-band neutrino beam on a fixed target:  $E_\nu = 80$  GeV,  $x = 0.1$ ,  $Q^2 = 10$  GeV<sup>2</sup>. We plot  $d\sigma$  in 2-dimensions *vs.*  $z$  and  $\eta$  in Fig. (2), and in Fig. (3) we show 1-dimensional slices for distinct bins in  $z$  plotted against  $\eta$ . Comparing Fig. (3)-a and Fig. (3)-b, we see the effect of the narrow- and wide-binning.

Finally, in Fig. (4), we show results for  $d\sigma_{\{x,y,z,\eta,Q^2\}}$  as defined by Eq. (15) for the case where either  $\eta$  or  $z$  is integrated out; again, we display this for fine-binnings of  $1 \times 100$  or  $100 \times 1$ , and broad-binnings of  $1 \times 5$  or  $10 \times 1$ .<sup>10</sup>

As expected, the negative Sudakov logarithms occur at large  $z$  where we have  $\eta \lesssim \eta_{\max}$  in the integrand.<sup>11</sup> This behavior is clearly evident in Fig. (3) where we see that in the case of fine binning (Fig. (3)-a) and large  $z$  (dotted curve, corresponding to  $z \in [0.95; 0.96]$ ), the  $\eta$ -distribution turns negative in the lowest rapidity bin. In contrast, in the case of broad binning (Fig. (3)-b) and large  $z$  (dotted curve, corresponding to  $z \in [0.8; 1]$ ), the  $\eta$ -distribution remains positive throughout the full  $z$ -range. Similarly, the  $z$ -distribution in (Fig. (4)-a) is rendered positively definite if the binning is broadened at large- $z$ . Hence, we observe that negative weights can be easily avoided by using sufficiently broad bins in a reasonable broadening of the binning

To summarize, we observe that the negative differential distributions arising from the negative Sudakov logarithms yield unphysical singular components present in our fixed-order result. When sufficiently broad bins are chosen, these singular components integrate out to yield a positive definite binned result. In an actual experimental analysis, this requirement of broad bins arises naturally given the finite detector resolution.

Our use of bins to regularize the differential distributions will have negligible impact on the experimental analysis because our bin size is small compared to the experimental detector resolution, even more so because the detector acceptance is a smooth function in terms of the set of kinematic variables. In particular, while the exact choice of bins is subject to any experimental analysis, the geometry of typical neutrino detectors as reflected in the acceptance functions of Fig. 1 demonstrates the effective experimental bin size in  $z$  and  $\eta$  is comfortably large enough for the purpose of regularizing the differential distributions with the binning technique.

To conclude this Section, let us note that in the lowest- $z$  curves of Fig. (3), one observes – apart from the forward peak at  $\eta \lesssim \eta_{\max}$  typical of an  $W s' \rightarrow c$  event – a broader backward plateau stemming from the scattering off a collinear (in the boson-target CMS) charm quark. For the fixed target kinematics under consideration, this backward peak is seen to be strongly suppressed compared to the forward peak. This observation gives us confidence that one is actually measuring the scattering off strange quarks, with only a small dilution from charm

---

<sup>10</sup>As an important cross-check on these results, we verify that the binning  $\eta \times z = 1 \times n$  (rapidity integrated out) reproduces the integrated results in the literature [16, 18]

<sup>11</sup>Due to our orientation of the  $z$ -axis along the target direction we denote  $\eta_{\max} \equiv \max(|\eta|) = \max(-\eta)$

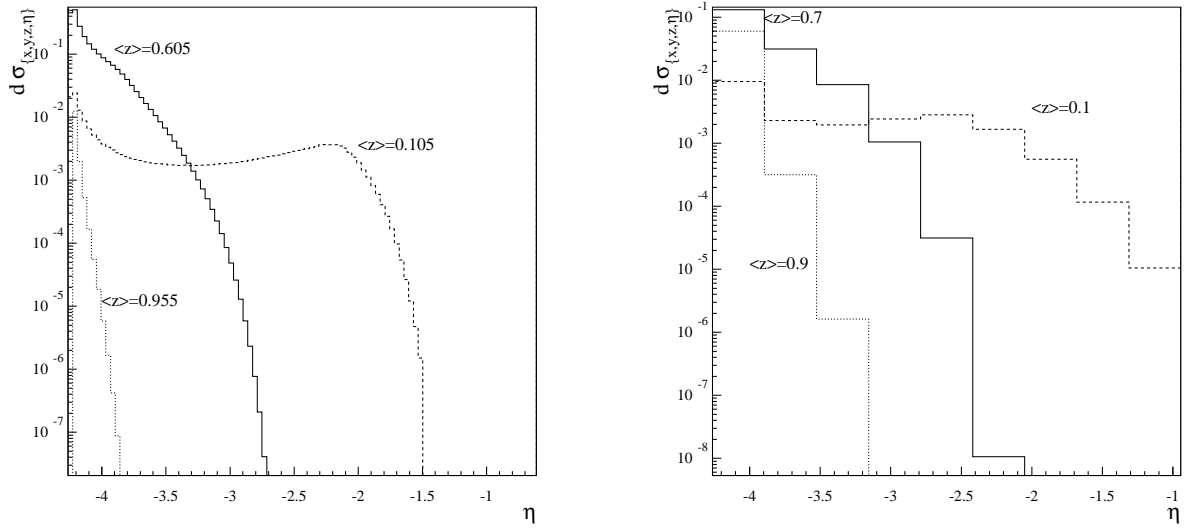


Figure 3: Binned differential distributions in the charm rapidity,  $\eta$ . Shown are results for a fine binning ( $100 \times 100$ ) in  $\eta \times z$  (left), and a broad binning (right) of  $10 \times 5$ . The fine-binned results refer to  $z$ -bins centered around 0.105, 0.605 and 0.955, respectively, while the broad-binned results refer to 0.1, 0.7 and 0.9.

quarks. Hence, this verifies the opposite sign dimuon data provides a direct determination of  $s(x, Q^2)$  at NLO level.

## 5 Conclusions

We have presented a fully differential NLO calculation of the neutrino-induced DIS charm production process. This calculation is an essential ingredient for a complete analysis of the dimuon data, and will allow a precise determination of the strange quark PDF. We have demonstrated that by binning the data appropriately, we can interface the theoretical calculation (containing  $\delta$ -functions and “plus-distributions”) directly to the experimental Monte Carlo analysis program. We observe the enhancement of the Sudakov logarithms at the phase-space boundaries, and verify that these can be controlled with this binning method.

The fully differential distributions obtained here allow charged current neutrino DIS experiments to use the complete NLO QCD result in the Monte Carlo data analysis.<sup>12</sup> These tools will allow us to extract the strange quark PDF from the dimuon data at NLO; this

<sup>12</sup>These results are available as a FORTRAN code, DISCO.

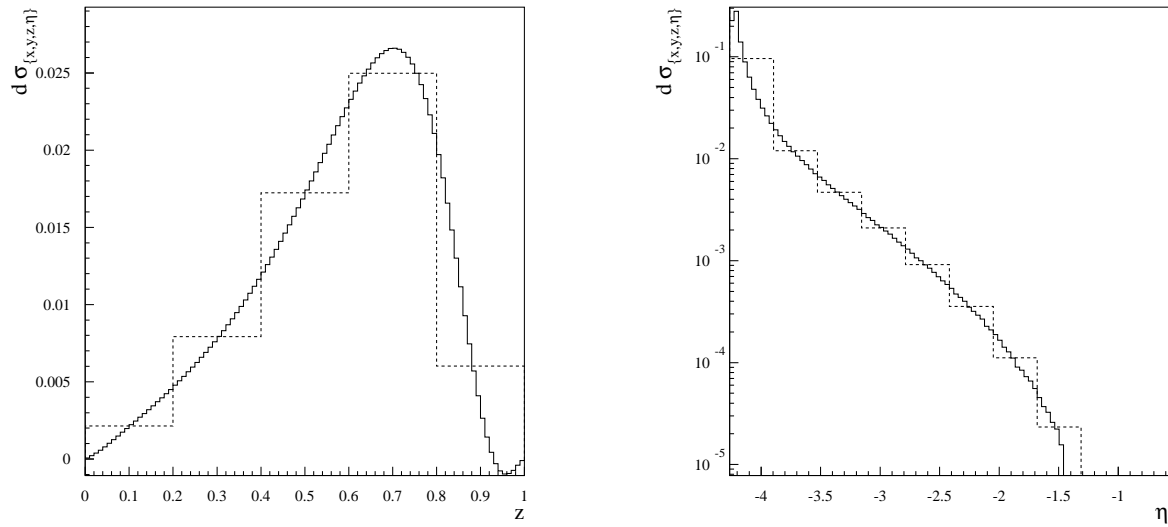


Figure 4: Binned distribution in  $z$  (left:  $\eta$  integrated out) and  $\eta$  (right:  $z$  integrated out), each for a fine and a broad binning.

information should prove crucial to resolving the unusual behavior of the strange quark in the proton.

## Acknowledgment

The Authors would like to thank T. Adams, T. Bolton, R. Frey, M. Goncharov, J. Morfin, R. Scalise, P. Spentzouris, and W.-K. Tung for helpful discussions. This research was supported by the National Science Foundation under Grant PHY-0070443, by the U.S. Department of Energy, and by the Lightner-Sams Foundation.



## References

## References

- [1] H. L. Lai *et al.* [CTEQ Collaboration], Eur. Phys. J. **C12**, 375 (2000)
- [2] M. Glück, E. Reya and A. Vogt, Eur. Phys. J. **C5**, 461 (1998).
- [3] A.D. Martin, R.G. Roberts, W.J. Stirling and R.S. Thorne, Eur. Phys. J. **C4**, 463, 1998.
- [4] V. Barone, C. Pascaud and F. Zomer, Eur. Phys. J. **C12**, 243 (2000).
- [5] S. Alekhin, Eur. Phys. J. **C10**, 395 (1999); W. T. Giele and S. Keller, Phys. Rev. D **58**, 094023 (1998); W. T. Giele, S. Keller and D. A. Kosower, “Parton distributions with errors,” *In \*La Thuile 1999, Results and perspectives in particle physics\* 255-261*; J. Pumplin, D. R. Stump and W. K. Tung, hep-ph/0008191, hep-ph/0101032, hep-ph/0101051.
- [6] S. Kretzer, F.I. Olness, R.J. Scalise, R.S. Thorne and U.K. Yang, Phys. Rev. **D64**, 033003 (2001).
- [7] J. Botts *et al.*, CTEQ1, Phys. Lett. **B304**, 159 (1993).
- [8] M. Glück, S. Kretzer and E. Reya, Phys. Lett. **B380**, 171 (1996); **B405**, 391 (1996) (E).
- [9] V. Barone, M. Genovese and N.N. Nikolaev, Z. Phys. **C70**, 83 (1996).
- [10] P. Vilain *et al.* [CHARM II Collaboration], Eur. Phys. J. **C11**, 19 (1999).
- [11] A. O. Bazarko *et al.* [CCFR Collaboration], Z. Phys. **C65**, 189 (1995); A. O. Bazarko, Ph.D. Thesis. NEVIS-1504
- [12] S.A. Rabinowitz *et al.* [CCFR Collaboration], Phys. Rev. Lett. **70**, 134 (1993).
- [13] H. Abramowicz *et al.* [CDHSW Collaboration], C. Phys. **C15**, 19 (1982).
- [14] P. Astier *et al.* [NOMAD Collaboration], Phys. Lett. **B486** (1990) 35.
- [15] M. Goncharov *et al.* [NuTeV Collaboration], Phys. Rev. **D64**, 112006 (2001).

- [16] M. Glück, S. Kretzer and E. Reya, Phys. Lett. **B398**, 381 (1997); **B405**, 392 (1997) (E).
- [17] U.K. Yang *et al.* [CCFR/NuTeV Collaboration], Phys. Rev. Lett. **86**, 2742 (2001).
- [18] S. Kretzer and M. Stratmann, Eur. Phys. J. **C10**, 107 (1999).
- [19] V. Barone, U. D'Alesio and M. Genovese, in proceedings of the 1995/96 workshop on 'Future Physics at HERA', Hamburg, 1996, G. Ingelman, A. De Roeck and R. Klanner (eds.), p. 102.
- [20] K. Ackerstaff *et al.* [HERMES Collaboration], Phys. Rev. Lett. **81**, 5519 (1998); Phys. Lett. **B464**, 123-134 (1999).
- [21] R.D. Ball, D.A. Harris, K.S. McFarland, proceedings of NuFACT'00 (*International Workshop on Muon Storage Ring for a Neutrino Factory, Monterey, California, 22-26 May 2000*), hep-ph/0009223; S. Forte, M.L. Mangano, G. Ridolfi, Nucl. Phys. **B602**, 585 (2001).
- [22] T. Gottschalk, Phys. Rev. **D23**, 56 (1981).
- [23] F. Olness, W.K. Tung, Nucl. Phys. **B308** (1988) 813; M. Aivazis, F. Olness, W.K. Tung, Phys. Rev. **D50** (1994) 3085; M. Aivazis, J.C. Collins, F. Olness, W.K. Tung, Phys. Rev. **D50** (1994) 3102.
- [24] R.S. Thorne, R.G. Roberts, Phys. Lett. **B421** (1998) 303; Phys. Rev. **D57** (1998) 6871; Eur. Phys. J. **C19** 339 (2001).
- [25] M. Krämer, F. Olness, D. Soper, Phys. Rev. **D62**, 096007 (2000).
- [26] S. Kretzer, I. Schienbein Phys. Rev. **D56** (1997) 1804; Phys. Rev. **D58** (1998) 094035; Phys. Rev. **D59** (1999) 054004.
- [27] M. Buza, W.L. van Neerven, Nucl. Phys. **B500**, 301 (1997).
- [28] H1 Collab. and ZEUS Collab. (Felix Sefkow for the collaboration); proceedings of 30th International Conference on High-Energy Physics (ICHEP 2000), Osaka, Japan, 27 Jul - 2 Aug 2000; hep-ex/0011034.
- [29] B.W. Harris and J. Smith, Nucl. Phys. **B452**, 109 (1995).
- [30] V. Barger, R.J.N. Phillips, Phys. Rev. **D14**, 80 (1976).

- [31] C. Peterson *et al.*, Phys. Rev. **D27**, 105 (1983).
- [32] Y. L. Dokshitzer, D. Diakonov and S. I. Troian, Phys. Rept. **58**, 269 (1980).
- [33] J. C. Collins, D. E. Soper and G. Sterman, Nucl. Phys. B **250**, 199 (1985).
- [34] H. Contopanagos and G. Sterman, Nucl. Phys. B **419**, 77 (1994) [hep-ph/9310313].
- [35] R. K. Ellis and S. Veseli, Nucl. Phys. B **511**, 649 (1998) [hep-ph/9706526].
- [36] M. Aguilar-Benitez *et al.* [LEBC-EHS Collaboration], Phys. Lett. B **123**, 103 (1983).
- [37] N. Ushida *et al.* [Fermilab E531 Collaboration], Phys. Lett. B **206**, 375 (1988); Phys. Lett. B **206**, 380 (1988);  
N. Ushida *et al.* [Canada-Japan-Korea-USA Hybrid Emulsion Spectrometer Collaboration], Phys. Lett. B **121**, 292 (1983).
- [38] P. Nadolsky, D.R. Stump and C.-P. Yuan, Phys. Rev. **D61** (2000) 014003, hep-ph/0012261.
- [39] M. Cacciari, S. Catani, Nucl. Phys. **B617**, 253 (2001).
- [40] L. Apanasevich *et al.*, Phys. Rev. D **59**, 074007 (1999) [hep-ph/9808467].
- [41] R. Meng, F. I. Olness and D. E. Soper, Phys. Rev. D **54**, 1919 (1996) [hep-ph/9511311].
- [42] F. Landry, R. Brock, G. Ladinsky and C. P. Yuan, Phys. Rev. D **63** (2001) 013004 [hep-ph/9905391]. C. Balazs and C. P. Yuan, Phys. Rev. D **56**, 5558 (1997) [hep-ph/9704258]. G. A. Ladinsky and C. P. Yuan, Phys. Rev. D **50**, 4239 (1994) [hep-ph/9311341].